Phase precipitation and magnetic properties in multi-alloying $Nd_2Fe_{14}B$/α-Fe nanocomposite magnets

ZHANYONG WANG[*], WENQING LIU[a], YANLI SUI[b]

Department of Materials Science and Engineering, Shanghai Institute of Technology, Shanghai 200235, China
[a]Institute of Materials Science, Shanghai University, Shanghai 200072, China
[b]State Key Laboratory for Advanced Metals and Materials, USTB, Beijing 100083, China

The $Nd_2Fe_{14}B$/α-Fe nanocomposite magnets multi-alloyed with Co, Nb, Zr and V were prepared by melt spinning. The grains with an average grain diameter of 20–30 nm in size shows extremely homogenous and regular characteristic. The remanence and coercivity reach to 80emu/g and 567kA/m, respectively for the ribbons annealed at 710^oC for 4 minutes. Three dimensional atom probe (3DAP) were applied to investigate the elemental distributions of V, Zr and Nb in annealed ribbons. V-enriched intergranular phase with complex characters was found at the grain boundaries.

1. Introduction

As preferred permanent magnets with potential properties, NdFeB-based nanocomposite magnets, including $Nd_2Fe_{14}B$/α-Fe and $Nd_2Fe_{14}B$/Fe_3B, have received much attention. The remanence and coercivity can be enhanced theoretically through the exchange coupling between magnetically hard and soft phases with grain in nano size [1,2]. Different methods modifying the composition or process have been applied to reach the theoretical magnetic properties as close as possible [3-10]. The bulk anisotropic nanocomposite magnets with optimum magnetic properties have been obtained by hot deformation at about 700 ℃ after the powders are densified by hot compactionv[10]. No matter what methods are applied, microalloying is necessary additional mean to modify the microstructure simultaneously. The single or combinatory substitutions of the Fe and/or Nd elements usually have significant effects on the improvement of magnetic properties and microstructure characteristics [11-20]. As mentioned in other reports, the single addition of refractory elements Nb, Zr and V is useful in controlling the grain size of both the a-Fe and $Nd_2Fe_{14}B$ phases in nanocomposite magnets for the precipitation of Nb-enriched, Zr-enriched and V-enriched phases at grain boundary [11]. However, the combined addition also plays more excellent roles in the microstructure modification and property enhancement [17, 18]. In this work, the $Nd_2Fe_{14}B$/α-Fe nanocomposite magnets multi-alloyed with Co, Nb, Zr and V were investigated and some interesting microstructure characters have been found in this alloy.

2. Experimental

The ingots with the composition of $Nd_{8.5}Fe_{77.1}B_{6.4}Co_4Zr_3Nb_{0.5}V_{0.5}$ were prepared with pure Nd, Fe, Co, Nb, Zr and V as raw materials by non-consumable arc-melting under purified argon atmosphere. The ingots were put into quartz tube with an orifice diameter about 0.7mm and melt-pun onto copper roll with wheel speed of 15m/s. The obtained ribbons were annealed at 710 ^oC for 4 minutes in the vacuum of $2\times10^{-3}Pa$. The structure of the annealed ribbons was identified by X-ray diffraction instrument (D/max-γB). TEM observation was carried out to investigate the microstructure by using JEM-200CX transmission electron microscopy. 3DAP (Three-dimensional atom probe) instrument was employed to investigate the elemental distribution. As an instrument for investigating the microstructure of materials by analyzing atoms one by one, 3DAP can map out elemental distribution in a nanometric volume with near atomic resolution. Atom probe analysis is performed at a tip temperature of about 65K under an ultra-high vacuum condition ($<1\times10^{-8}Pa$) with a pulse fraction (a ratio of pulse voltage to the static voltage) of 0.15 and a pulse repetition rate of 500 Hz. The thermo-gravimetry analysis (TGA) between 20~500 ℃ was employed using TA 2050 (TA Instrument) at a heating rate of $10℃.min^{-1}$. The magnetic properties of the ribbons were measured along the spun direction by VSM with maximum applied magnetic field of 1.8 T.

3. Results and discussion

Fig.1 shows XRD spectrum of $Nd_{8.5}Fe_{77.1}B_{6.4}Co_4Zr_3Nb_{0.5}V_{0.5}$ ribbons annealed at 710℃ for 4 min. The sample displays a mixture of magnetically hard $Nd_2Fe_{14}B$ phase and soft a-Fe phase with the low volume fraction of a-Fe and without obvious metastable phase. Comparing the stoichiometric of single $Nd_2Fe_{14}B$ phase ($Nd11.76Fe82.35B5.88$) with the normal composition of the sample, the rare earth content in the sample is much lower and there are excess Fe and B according to the stoichiometric of $Nd_2Fe_{14}B$. However the diffraction peaks of a-Fe phase are not such strong enough as reported by Yang [19] and Cui [20]. So the micro-alloyed elements should play an important role in the phase constitute of the sample and the excess Fe and B, combining with the micro-alloyed elements, perhaps transforms into other phases. Fig.2 is the TEM micrographs of ribbons annealed at 710℃ for 4 min. The grains with an average grain diameter of 20–30 nm in size shows extremely homogenous and regular characteristic, which enhances the interaction coupling between grains and improves the magnetic properties, especially the squareness of Hysteresis loop, as shown in Fig.3. The remanence and coercivity reach to 80emu/g and 567kA/m, respectively, similar to the magnetic properties of Nb, Zr-bearing ribbons [21].
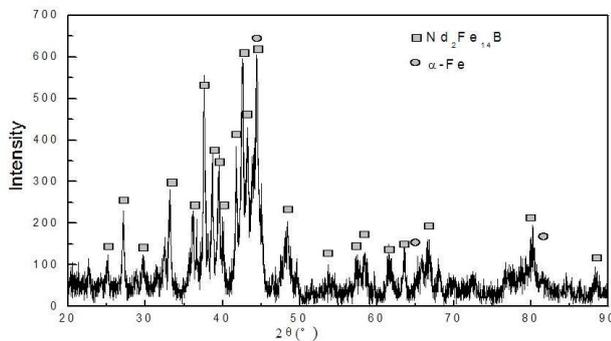
Fig.1 XRD spectrum of the $Nd_{8.5}Fe_{77.1}B_{6.4}Co_4Zr_3Nb_{0.5}V_{0.5}$ ribbons annealed at 710 ᵒC for 4 min
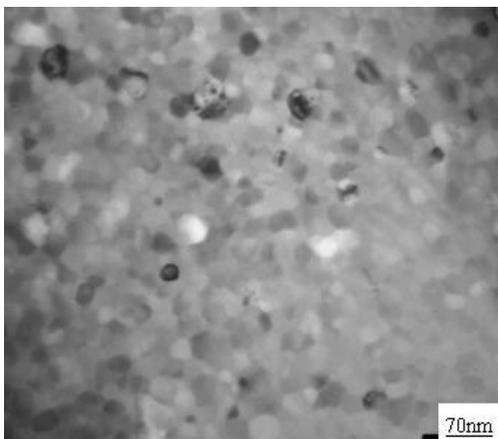
Fig.2 TEM micrographs of $Nd_{8.5}Fe_{77.1}B_{6.4}Co_4Zr_3Nb_{0.5}V_{0.5}$ ribbons annealed at 710℃for 4 min
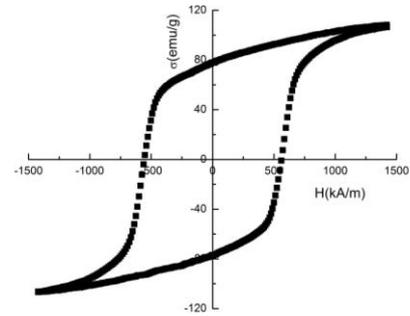
Fig.3 Hysteresis loops of $Nd_{8.5}Fe_{77.1}B_{6.4}Co_4Zr_3Nb_{0.5}V_{0.5}$ ribbons annealed at 710 ℃ for 4 min.

Table 1 The mass to charge ratio (m/Q) of each element in $Nd_{8.5}Fe_{77.1}B_{6.4}Co_4Zr_3Nb_{0.5}V_{0.5}$ alloy.

Element	Charge	Mass to charge ratio
Nd	3+, 2+	47.3, 47.7, 48, 48.3, 48.7, 49.3, 50,71, 71.5, 72, 72.5, 73, 74, 75
Fe	2+, 1+	27, 28, 28.5, 29, 54, 56, 57, 58
B	1+, 2+	10, 11, 5, 5.5
Co	2+, 1+	29.5, 59
Zr	2+, 3+	45, 45.5, 46, 47, 48, 30, 30.3, 30.7, 31.3, 32
Nb	2+, 3+	46.5, 31
V	2+, 3+	25.5, 17

To understand the formation of fine microstructure, three dimensional atom probe (3DAP) were applied to investigate the elemental distributions of V, Zr and Nb in annealed ribbons. The elemental distributions can be determined by both the mass to charge ratio (m/Q) and the position of ions at the same time. Table 1 shows the mass to charge ratio (m/Q) of each element in this alloy. Each element has two or more mass to charge ratio (m/Q) because of the different charge or isotope. On the Basis of table 1, the mass spectrum can be obtained, as shown in Fig.4. It can be found that the impurity of Mn, Si, C and Cr also can be distinguished even if their low concentration.
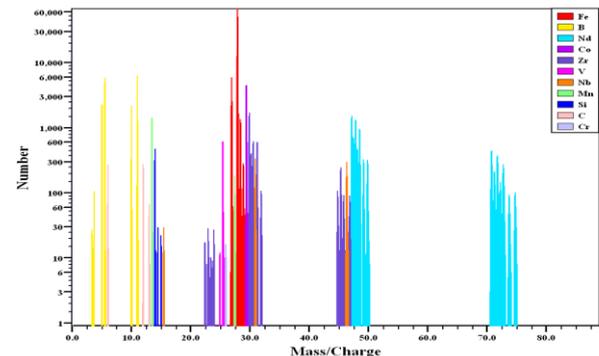
Fig.4 Mass spectrum of 3DAP for $Nd_{8.5}Fe_{77.1}B_{6.4}Co_4Zr_3Nb_{0.5}V_{0.5}$ alloy
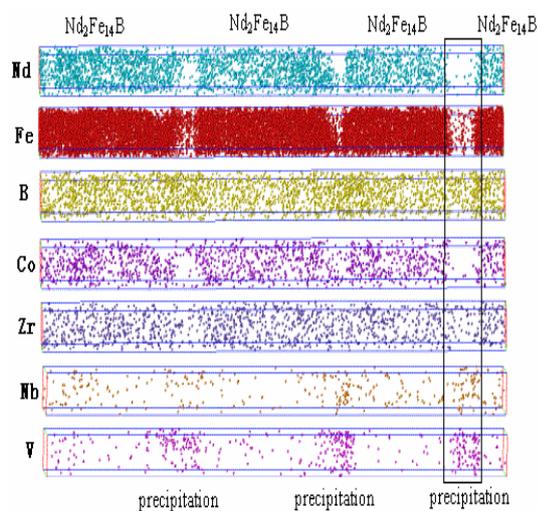
(a)3nm×3nm×50nm
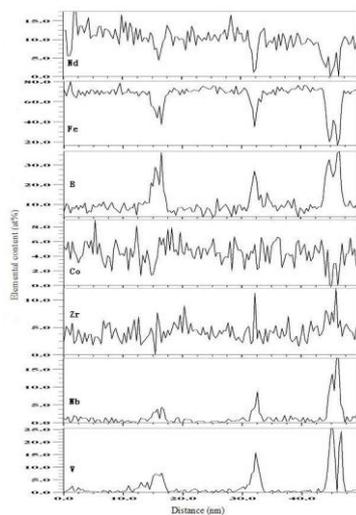
(b)

Fig. 5. The distribution of atom maps (a) and the corresponding concentration depth profiles (b) of the elements for $Nd_{8.5}Fe_{77.1}B_{6.4}Co_4Zr_3Nb_{0.5}V_{0.5}$ annealed alloy in a volume of 3nm×3nm×50nm

Fig.5 a and b show the distribution of atom maps and the corresponding concentration depth profiles of the elements for $Nd_{8.5}Fe_{77.1}B_{6.4}Co_4Zr_3Nb_{0.5}V_{0.5}$ annealed alloy in a volume of 3nm×3nm×50nm. V atoms have severer segregation than other elements, as well as Nb, B and Zr atoms (each dot represents one atom position), as shown in Fig.5a. Significant concentration changes can be found in some regions from Fig.5b. The concentrations of V, Nb and B atoms in these regions are almost many times of the other regions, as well as the poor concentrations of Nd and Fe atoms. Zr atoms also have slight enrichment at these regions. It is worth mentioned that the composition of these regions is close to (V,Nb,Zr)30Fe40B30, different from the results of Wu [22]. According to the composition of the regions between the precipitations, the Nd, Fe and B concentrations are almost similar to the stoichiometric of

$Nd_2Fe_{14}B$ phase, so the phase in theses regions is believed to be $Nd_2Fe_{14}B$ phase, which is the main phase from the XRD patterns. There are few V and Nb atoms in $Nd_2Fe_{14}B$ phase.
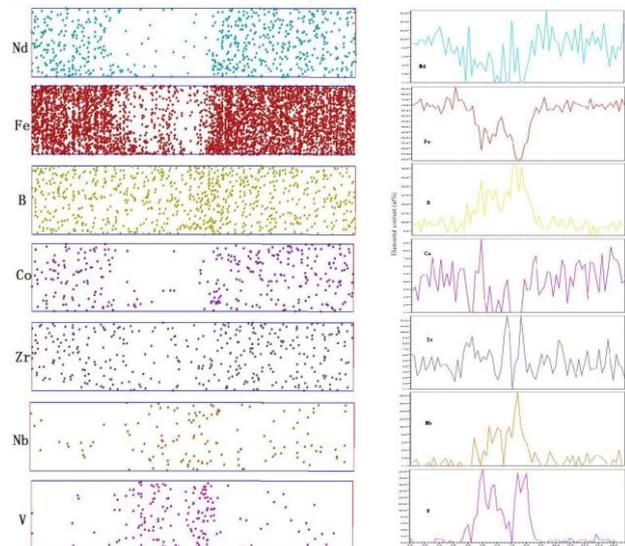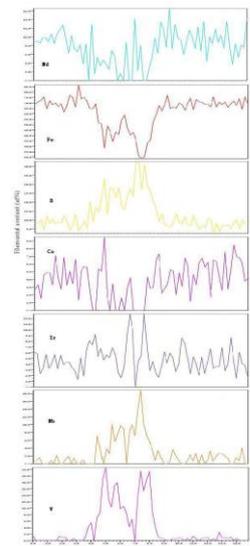
(a)3nm×3nm×15nm   (b)
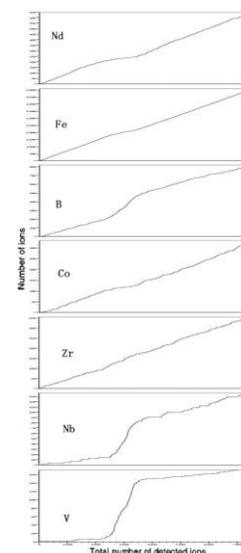
(c)

Fig. 6. The distribution of atom maps (a), the corresponding concentration depth profiles (b), and the corresponding integral depth profiles (c) of the elements for $Nd_{8.5}Fe_{77.1}B_{6.4}Co_4Zr_3Nb_{0.5}V_{0.5}$ annealed alloy in a volume of 3nm×3nm×15nm

It should be mentioned that the Nb and V atoms have very similar distribution except for small difference. Fig.6 shows the distribution of atom maps, the corresponding concentration depth profiles and the corresponding integral depth profiles of the elements in a selected region near the Nb-V-enriched region (marked in Fig.5a). In this region, Fe atoms also distributes heterogeneously. At the boundary

of $Nd_2Fe_{14}B$ phase, there is a thin layer with the Fe and B concentrations similar to the stoichiometric of Fe_3B phase. The thickness of this thin layer is about 0.5 nm, which make it difficult to distinguish its phase structure. Slight enrichment of Nb and V atoms also can be found in this region. As reported by Xiong [23], the concentration for vanadium atoms partition into the soft magnetic phase Fe_3B is only about 5 at%, lower than the concentration shown in Fig.6 b. So the phase in this region can not be determined to be Fe_3B phase. While the concentration ratio of refractory elements (Zr, Nb and V), Fe and B at the center of the precipitation is close to 1:1:1, similar to the composition of precipitations in $Nd_2Fe_{14}B/\alpha$-Fe nanocomposite magnets microalloyed with 5% Nb [24]. The corresponding integral depth profiles are presented in Fig. 6c. The slope of the plot corresponds to the local solute concentration. The concentration variety between the hard magnetic grains also can be found obviously.
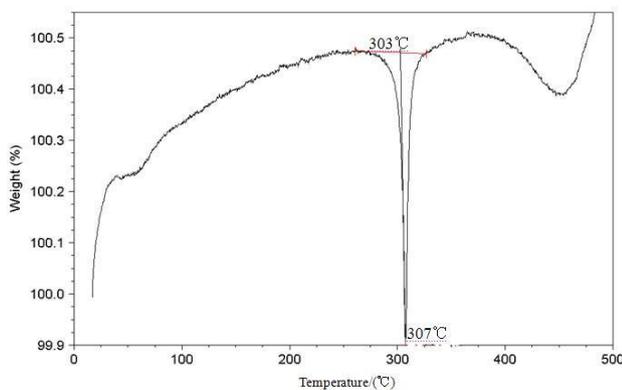
Fig.7 DTG curve of 3DAP for $Nd_{8.5}Fe_{77.1}B_{6.4}Co_4Zr_3Nb_{0.5}V_{0.5}$ alloy

From the above results, it can be found that V has much higher tendency to segregate at grain boundary than other elements, i.e, Nb and Zr. The precipitation of V-enriched phase and the dissolution of V in $Nd_2Fe_{14}B$ phase are helpful to suppress the growth of grains and control the micro morphology. So with the co-addition of V, Nb and Zr, a homogeneous, fine microstructure has been obtained, which enhances the interaction coupling between grains and improves the magnetic properties. The existence of V-enriched phase between hard magnetic $Nd_2Fe_{14}B$ phases prevents direct contact of hard magnetic phases, which leads to the increase of coercivity. The Curie temperature for this composite magnets has not change significantly due to the dissolution of V and Nb atoms in $Nd_2Fe_{14}B$ phase [23], as shown in Fig.7.

4. Conclusion

The combined addition of Co, Nb, Zr and V has great effects on microstructure and magnetic properties of

$Nd_2Fe_{14}B/\alpha$-Fe nanocomposite magnets. Co atoms have the same distribution characters with Fe atoms. V and Nb atoms dissolute in $Nd_2Fe_{14}B$ phase and segregate at grain boundary. While Zr atoms show slight enrichment at the edge of the $Nd_2Fe_{14}B$ phase. At the boundary of $Nd_2Fe_{14}B$ phase, there is a thin layer with the Fe and B concentrations similar to the stoichiometric of Fe_3B phase with thickness of 0.5 nm. The concentration ratio of refractory elements (Zr, Nb and V), Fe and B at the center of the precipitation is close to 1:1:1. The Curie temperature has not change significantly due to the dissolution of V and Nb atoms in $Nd_2Fe_{14}B$ phase.

Reference

[1] R. Skomski, J.M.D. Coey, Phys. Rev. B. **48**,15812(1993).
[2] T.Schrefl, R.Fischer, J.Fidler, H. Kronmuller, J. Appl. Phys. **76**,7053(1994).
[3] C. Y. You, X. K. Sun, L. Y. Xiong, W. Liu, B. Z. Cui, X. G. Zhao, D. Y. Geng, Z. D. Zhang, J Magn. Magn. Mater. **268**, 403(2004).
[4] Yanguo Liu, Lei Xu, Qingfeng Wang, Wei Li, Xiaohong Li, Yanwu Xie, Xiangyi Zhang, Mater. Lett. **62**, 3890(2008).
[5] Zhanyong Wang, Hui Xu, Jiansen Ni, Qiang Li, Bangxin Zhou, Rare Metals, **25**, 337(2006).
[6] S. Hirosawa, H. Kanekiyo, Y. Shigemoto, K.Murakami, T.Miyoshi, Y.Shioya, J Magn. Magn. Mater. **239**, 424(2002).
[7] B.Z.Cui, M.Q. Huang, R.H. Yu, J. Appl. Phys. **93**,8128 (2003).
[8] J.F Liu, H.A Davies, J Magn. Magn. Mater. **157-158**, 29(1996).
[9] S Gutoiu, E Dorolti, O Isnard, I Chicinas, V Pop, J. Optoelectron. Adv. Mater. **12**, 2126(2010).
[10] D. Lee, J.S. Hilton, C.H. Chen, Y Zhang, G C Hadjipanayis, S Liu, IEEE Trans. Magn. **40**, 2904 (2004).
[11] K. Hono, Prog. Mater. Sci. **47,** 621 (2002).
[12] Choong Jin Yang, Jong Soo Han, Eon Byeung Park, Eng Chan Kim, J. Magn. Magn. Mater. **301**, 220(2006).
[13] S.Y. Zhang, H. Xu, J.S. Ni, H.L. Wang, X.L. Hou, Y.D. Dong, Physica B: Condensed Matter. **393**, 153(2007).
[14] Z.M. Chen, Y.Q Wu, M.J Kramer, B.R. Smith,

B.M. Ma, M.Q. Huang, J Magn Magn Mater. **268**, 105(2004).

[15] H.W. Chang, M.F. Shih, C.C. Hsieh, W.C. Chang, J. Alloys Compd. **484**,143(2009).

[16] Yanli Sui, Zhanyong Wang, Maocai Zhang, Shouzeng Zhou, J. Magn. Magn. Mater. **321**, 3974 (2009).

[17] Sen Yang, Xiaoping Song, Shandong Li, Xiansong Liu, Zongjun Tian, Benxi Gu, Youwei Du, J. Magn. Magn. Mater. **263**,134 (2003).

[18] D.H. Ping, K. Hono, H. Kanekiyo, S. Hirosawa, Acta mater, **47**, 4641 (1999).

[19] Sen Yang, Shandong Li, Xiansong Liu, Xiaoping Song, Benxi Gu, Youwei Du. J. Alloys Compd. **343**,217 (2002).

[20] B.Z. Cui, X.K. Sun, W. Liu, Z.D. Zhang, D.Y. Geng, X.G. Zhao, J.P. Liu, David J. Sellmyer. J. Appl. Phys. **87**,5355(2000).

[21] Zhanyong Wang, Wenqing Liu, Bangxin Zhou, Jiansen Ni, Hui Xu, J. Iron Steel Res. Int. **13**,183 (2006).

[22] Y.Q. Wu, H. Yamamoto and K. Hono, Scripta mater. **44**, 2399 (2001).

[23] X.Y. Xiong, K. Hono, S. Hirosawa, H. Kanekiyo, J. Appl. Phys. **91**, 9308 (2002).

[24] Zhanyong Wang, Wenqing Liu, Bangxin Zhou, Jiansen Ni, Hui Xu, Yongzheng Fang, Minglin Jin, Physica B: Condensed Matter. **404**,1321 (2009).

_____

*Corresponding author: zhanyong.wang@vip.sina.com